

A weak electric field-assisted ultrafast electrical switching dynamics in In_3SbTe_2 phase-change memory devices

Cite as: AIP Advances 7, 075206 (2017); <https://doi.org/10.1063/1.4994184>

Submitted: 17 April 2017 . Accepted: 03 July 2017 . Published Online: 13 July 2017

Shivendra Kumar Pandey, and Anbarasu Manivannan



View Online



Export Citation



CrossMark

ARTICLES YOU MAY BE INTERESTED IN

[Sub-nanosecond threshold-switching dynamics and set process of \$\text{In}_3\text{SbTe}_2\$ phase-change memory devices](#)

Applied Physics Letters **108**, 233501 (2016); <https://doi.org/10.1063/1.4953196>

[A fully automated temperature-dependent resistance measurement setup using van der Pauw method](#)

Review of Scientific Instruments **89**, 033906 (2018); <https://doi.org/10.1063/1.4998340>

[An ultrafast programmable electrical tester for enabling time-resolved, sub-nanosecond switching dynamics and programming of nanoscale memory devices](#)

Review of Scientific Instruments **88**, 123906 (2017); <https://doi.org/10.1063/1.4999522>



Call For Papers!

AIP Advances

SPECIAL TOPIC: Advances in Low Dimensional and 2D Materials

A weak electric field-assisted ultrafast electrical switching dynamics in In_3SbTe_2 phase-change memory devices

Shivendra Kumar Pandey¹ and Anbarasu Manivannan^{1,2,a}

¹*Discipline of Electrical Engineering, Indian Institute of Technology Indore, Indore 453552, Madhya Pradesh, India*

²*Metallurgical Engineering and Materials Science, Indian Institute of Technology Indore, Indore 453552, Madhya Pradesh, India*

(Received 17 April 2017; accepted 3 July 2017; published online 13 July 2017)

Prefixing a weak electric field (incubation) might enhance the crystallization speed via pre-structural ordering and thereby achieving faster programming of phase change memory (PCM) devices. We employed a weak electric field, equivalent to a constant small voltage (that is incubation voltage, V_i of 0.3 V) to the applied voltage pulse, V_A (main pulse) for a systematic understanding of voltage-dependent rapid threshold switching characteristics and crystallization (*set*) process of In_3SbTe_2 (IST) PCM devices. Our experimental results on incubation-assisted switching elucidate strikingly one order faster threshold switching, with an extremely small delay time, t_d of 300 ps, as compared with no incubation voltage ($V_i = 0$ V) for the same V_A . Also, the voltage dependent characteristics of incubation-assisted switching dynamics confirm that the initiation of threshold switching occurs at a lower voltage of 0.82 times of V_A . Furthermore, we demonstrate an incubation assisted ultrafast *set* process of IST device for a low V_A of 1.7 V (~18 % lesser compared to without incubation) within a short pulse-width of 1.5 ns (full width half maximum, FWHM). These findings of ultrafast switching, yet low power *set* process would immensely be helpful towards designing high speed PCM devices with low power operation. © 2017 Author(s). All article content, except where otherwise noted, is licensed under a Creative Commons Attribution (CC BY) license (<http://creativecommons.org/licenses/by/4.0/>). [<http://dx.doi.org/10.1063/1.4994184>]

I. INTRODUCTION

In the recent years, chalcogenide-based phase change memory (PCM) have substantiated their ability for the next generation high-speed, non-volatile memory and also towards ‘*universal memory*’ for future computing systems.^{1–5} This is primarily owing to its all-round characteristics such as high read/write speeds, low power consumption, longer endurance, high scalability and non-volatile nature.^{6,7} The heart of this memory concept lies in the fascinating property-portfolio of rapid and reversible switching between a high resistivity amorphous (*reset*) state and a low resistivity crystalline (*set*) state on a nano/picosecond (ns/ps) timescale triggered by appropriate voltage pulses.^{2,3} However, the overall programming speed of PCM devices is particularly limited by the *set* process which is slower as compared to the *reset* process.⁸ This is primarily due to the fact that the *set* process is essentially governed by a combined effect of both the voltage-dependent ultrafast threshold switching dynamics exemplified by electronic effects,^{9–12} and rapid crystallization of phase change (PC) material induced by Joule heating.^{3,13} Hence, these two factors must be extensively investigated together to improve the speed of *set* operation. More importantly, another key factor of a correlation between the speed of *set* process and thermal stability of amorphous phase (governing data retention) must be discerned to overcome the speed limits of PCM devices.^{4,14}

^aElectronic mail: anbarasu@iiti.ac.in

In recent years, tremendous technological efforts have been devoted to improve the programming characteristics, structural stability, reliability and performance of PCM devices.^{6,7,15} However, achieving an ultrafast, yet low power threshold switching and crystallization using time-resolved measurements is a key challenge. Much recently, the crystallization/re-amorphization speed was achieved in 500 ps in $\text{Ge}_2\text{Sb}_2\text{Te}_5$ cells by means of a weak electric field induced switching.⁴ This technique offers an extremely fast crystallization through incubation-assisted thermal prestructural ordering, owing to faster nucleation and growth process as manifested by an ultrafast *set* process in 500 ps. However, such measurements lack the evidence of time-resolved data of current-voltage characteristics, which could possibly unveil a systematic enhancement over threshold switching and crystallization speed.

In addition to this, $\text{Ge}_2\text{Sb}_2\text{Te}_5$ material offers relatively poor thermal stability as reflected by a low crystallization temperature, T_c (~ 160 °C) which affects data retention.¹⁶ It has been recently reported that In_3SbTe_2 (IST) possesses an improved thermal stability as compared to the GeSbTe alloys. This is validated by the higher crystallization temperature (above 250 °C) of IST, which favours long-term data retention.¹⁷⁻¹⁹ In addition, IST material possesses a rock-salt type electronic structure similar to that of GeSbTe materials confirming rapid crystallization process of IST materials.²⁰ Also, the resistivity contrast of more than six orders of magnitude between the poly-crystalline and the amorphous phase of IST material, even promises multi-bit data storage applications.^{21,22} Moreover, very recently a systematic study of voltage-dependent threshold-switching dynamics and *set* process was demonstrated in IST cells in sub-ns timescale using an advanced custom-built programmable electrical tester.²³ Therefore, in the present study of incubation-assisted ultrafast switching, we have chosen IST material owing to its excellent thermal stability as well as fast electrical switching characteristics.

We report here, incubation-assisted ultrafast and low power threshold switching dynamics and *set* process of IST cells using time-resolved measurements. Our experimental findings of a weak electric field-assisted switching reveals at least one order faster threshold switching (i.e delay time of 300 ps) as well as *set* process for even 0.82 times of applied voltage, V_A with the pulse width of 1.5 ns (full width half maximum, *FWHM*). Also, we demonstrate a comparative analysis of switching speed upon systematic increment in V_A using the current-voltage characteristics in case of with and without incubation voltage in sub-ns timescale.

II. EXPERIMENTAL DETAILS

For a reliable exploration of such time-resolved ultrafast electrical switching measurements, an advanced electrical tester is essential with the capability of handling electrical signals in ps timescale. Hence, for the present study, we employed a custom-built programmable electrical tester (PET)^{11,23} having the ability to measure electrical signals precisely with a resolution of 50 ps and to capture switching transitions of devices in 200 ps. The PET setup consists of an Arbitrary Waveform Generator (AWG, *Agilent technologies*), a Digital Storage Oscilloscope (DSO, *Teledyne Lecroy*), custom-designed high frequency contact-boards having impedance-matching circuit (IMC) and amplifier (Amp) circuits specially designed with the intent to support electrical pulse measurements in the ps-timescale as described elsewhere.^{11,23} The pulse generator allows voltage pulses down to a pulse-width of 1.5 ns (*FWHM*), rise time, t_r , and fall time, t_f , of 1 ns having an amplitude up to 5 V.

In the present study, thin IST films were RF sputter-deposited from a single In_3SbTe_2 stoichiometric target (*ACI Alloys Inc.*) of 99.99 % purity operating in constant power mode of 25 W with a background pressure of 2.5×10^{-7} mbar, Ar flow of 20 s.c.c.m, and deposition rate of 0.0161 nm.s^{-1} . The SiO_2 substrates were kept under the rotation of 10 rpm to ensure homogeneity of the deposited films. The amorphous nature of the as-deposited thin IST films was confirmed by X-ray diffraction (XRD). The composition analysis of as-deposited IST films was performed by energy dispersive X-ray spectroscopic (EDS) technique at over five different locations, which confirms variations within 2 atomic percentages. Furthermore, the IST cells were fabricated on SiO_2 substrates using a 52 nm thick IST material as an active layer, sandwiched between the bottom electrode (*BE*, thickness of 30 ± 0.2 nm) and the top electrode (*TE*, thickness of 30 ± 0.2 nm) of Titanium (*Ti*). Mechanical masks were used for creating specific device patterns in a cross-bar like configuration such that the *BE* line width is 700 μm and a short *TE* line width is 300 μm as described elsewhere.^{11,23}

III. RESULTS AND DISCUSSION

The incubation-assisted electrical switching dynamics and *set* process of several IST cells were characterized in the as-deposited amorphous ($\sim 10 \text{ M}\Omega$) phase using the PET setup. We used pulse pattern comprising a plateau time, t_p of 100 ns, t_r and t_f of 1 ns. Fig. 1(a) displays the waveforms of main applied voltage pulse, V_A of both types, namely V_A with a small field incubation voltage, $V_i = 0.3 \text{ V}$ (right panel) and V_A without incubation voltage, $V_i = 0 \text{ V}$ (left panel). Fig. 1(b) shows the time-resolved current-voltage characteristics of IST cells for V_A of 1.4 V without incubation voltage (i.e. $V_i = 0 \text{ V}$) indicating no threshold switching, as evidenced by almost no current flow through the device. On the other hand, it is interesting to note from Fig. 1(c) that the device exhibit switching for

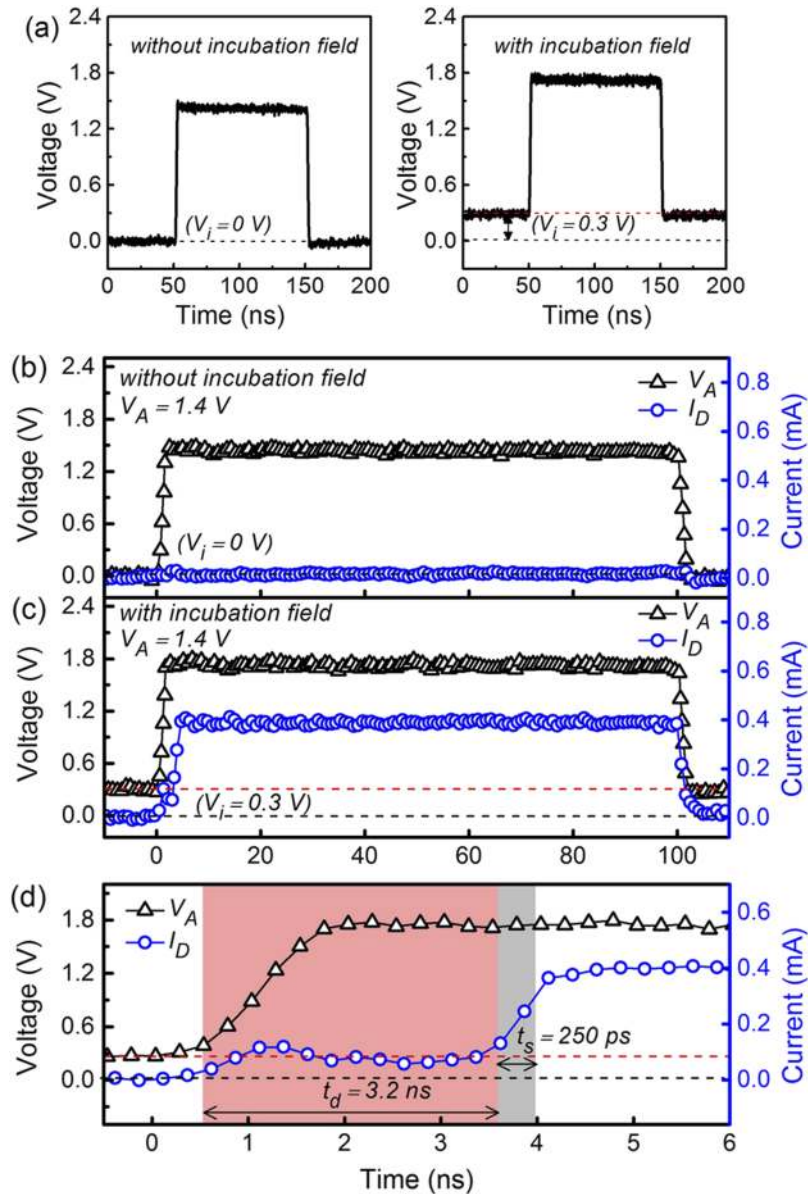


FIG. 1. (a) The waveforms of applied voltage pulse, V_A with a small field incubation voltage, $V_i = 0.3 \text{ V}$ (right) and without incubation voltage, $V_i = 0 \text{ V}$ (left). (b) Current-voltage characteristics for V_A of 1.4 V (black color, triangle), without incubation voltage ($V_i = 0 \text{ V}$) having plateau time of 100 ns, rise time and fall time of 1 ns. No significant increase in device current, I_D (blue color, circle) was observed. (c) Current-voltage characteristics for V_A of 1.4 V, with V_i of 0.3 V for the same pulse parameters revealing threshold switching as evidenced by a rapid increase in I_D from a-off to the conducting state (d) Enlarged view of transient characteristics depicting delay time, $t_d \sim 3.2 \text{ ns}$ and switching time, $t_s \sim 250 \text{ ps}$.

the same V_A of 1.4 V, with an incubation voltage ($V_i = 0.3$ V). It can be seen that the presence of a small field V_i of 0.3 V along with the same V_A (of 1.4 V) enables threshold switching after a finite delay time, t_d (the time elapsed prior to initiation of switching) as depicted by a rapid rise in the current through the device leading to conducting state. Subsequent to this, a *read* pulse (with amplitude of 0.2 V, pulse-width of 100 ns) confirms the permanent change from amorphous to a poly-crystalline state revealing *set* process of IST devices. Furthermore, in order to quantify transient parameters such as t_d of 3.2 ns and switching time, t_s of 250 ± 50 ps (current rise from amorphous off-to-on state), an enlarged view of the threshold switching process is shown in Fig. 1(d). It is noteworthy to mention here that the presence of incubation voltage ($V_i = 0.3$ V) with a main pulse V_A having an amplitude of 1.4 V enables electrical switching and *set* process.

In order to understand the effects of incubation voltage on the dependency of transient parameters including t_d , and t_s , we used various V_A by systematically varying the pulse amplitudes from 1.0 V to 2.3 V having the pulse parameters t_r , and t_f of 1 ns and t_p of 100 ns for both cases (i.e. with and without V_i). Fig. 2 displays the device current, I_D measured for varying V_A from 1.0 V to 2.3 V for both cases such that $V_i = 0$ V (as marked in black line) and $V_i = 0.3$ V (as marked in grey line). It is very interesting to note that IST devices exhibit switching from a significantly lower V_A of 1.4 V under incubation field, below which the device remains in the high resistance amorphous off (*a-off*) state. On the other hand, in the case of no incubation field, the device exhibits switching at a higher V_A of 1.7 V.

The precise values of t_d and t_s for various V_A of both with and without incubation, are actually estimated from Fig. 2 and are plotted in Fig. 3(a) and (b) respectively. Figure 3(a) depicts the dependence of t_d upon V_A for both cases, with and without incubation voltage, revealing the trend of an exponential decrease of t_d for increasing V_A . Such behaviour is in conformance with the previous reports; however, the present experiments manifest one order lower value of t_d as compared to other PC materials.^{8,10,15,24} Furthermore, it is noteworthy to mention here that incubation-assisted switching characteristics unravel a strikingly small value of t_d of 300 ± 50 ps for a lower V_A of 1.7 V (i.e. 0.82 times of V_A compared to without incubation). This finding corroborates that the incubation-assisted switching offers approximately one order smaller value of t_d , revealing a remarkable threshold switching speed of 300 ± 50 ps of IST devices, which is about one order faster than that of without incubation voltage. Moreover, the dependency of t_d , and threshold switching field (E_T) of IST devices were found to be in good-agreement with the literature.²³

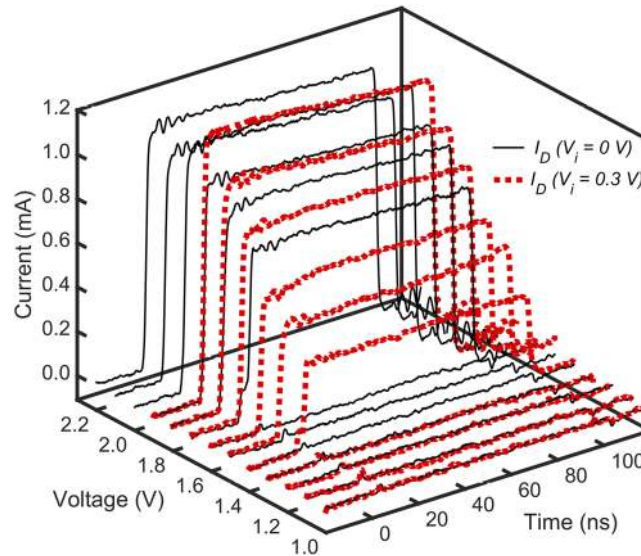


FIG. 2. Time-resolved measurement of the device current, I_D for applied voltage pulses, V_A ranging from 1.0 to 2.2 V for both cases such as without incubation voltage, $V_i = 0$ V (black color, solid lines) and also with incubation voltage, $V_i = 0.3$ V (red color, dashed lines). Initiation of switching is observed at V_A of 1.4 V with V_i of 0.3 V. On the other hand, switching is seen at higher V_A of 1.7 V in the case of without incubation voltage. The overlay of I_D reveals the dependency of transient parameters such as delay time, t_d and switching time, t_s .

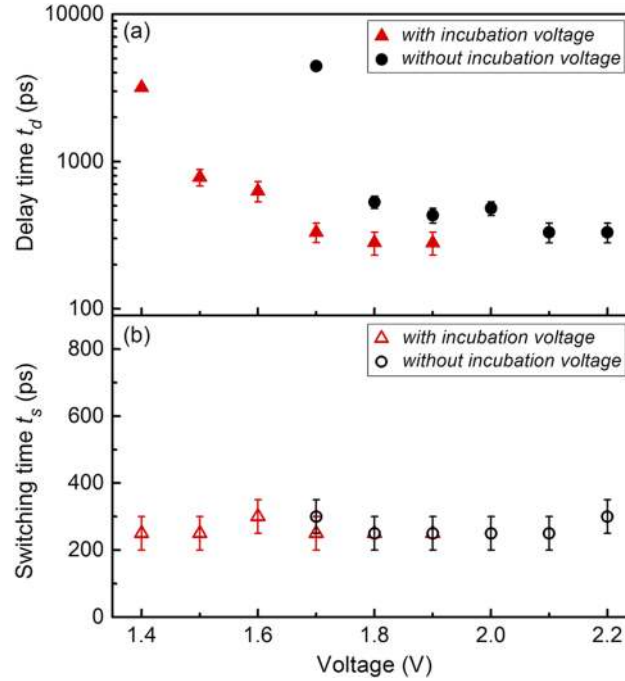


FIG. 3. (a) Dependence of delay time, t_d , and (b) switching time, t_s , on applied voltage pulse, V_A for both the cases of with (V_i of 0.3 V) and without incubation voltage (V_i of 0 V).

Furthermore, t_s is found to be a constant value at 250 ps for the application of various V_A , for both cases as depicted in Fig. 3(b). We found that the incubation voltage, although with a very small amount of thermal energy it delivers to the amorphous phase, can substantially enhance the speed of threshold switching by one order of magnitude, yet enabling low power switching of at least 0.82 times of V_A . Therefore, the scheme of incubation-assisted switching and the dependence of t_d upon V_A would be immensely helpful in optimization of pulse parameters towards programming of PCM devices in ps-timescale.

The approach of incubation-assisted switching process, by providing a weak electric field ($V_i = 0.3$ V) is known to induce thermal pre-structural ordering in the amorphous matrix,^{4,25,26} which eventually enhances the switching dynamics as well as induces the faster *set* process. In order to investigate the effect of incubation assisted ultrafast *set* process by employing our experimental data of voltage dependent transient parameters as described in Fig. 3, we have chosen a voltage pulse with a very short pulse-width (FWHM) of 1.5 ns, amplitude of 1.7 V, t_r , and t_f of 1 ns. It can be clearly seen from Fig. 3(a) that t_d for the V_A of 1.7 V is approximately 250 ps (for $V_i = 0.3$ V) and 5 ns (for $V_i = 0$ V). Therefore, it is presumed that in the case of no incubation voltage, owing to its higher t_d of 5 ns, the device does not exhibit switching within a very short pulse-width of 1.5 ns, for V_A of 1.7 V. And, the same is therefore; experimentally evident from Fig. 4(a) that the device does not show switching for the V_A of 1.7 V with a very short pulse-width of 1.5 ns. On the other hand, in the presence of incubation voltage, it is remarkable to note that the device exhibits switching from a high resistance *a-off* state to a conducting state after a very short t_d of 300 ps for the same V_A of 1.7 V having a very short pulse-width of 1.5 ns as depicted in Fig. 4(b). Subsequently, the current flowing through conducting state crystallizes the local region and therefore, the formation of a permanent low resistance state during the trailing edge of V_A leads to a very fast *set* operation. The *read* pulse (with amplitude of 0.2 V, pulse-width of 100 ns) confirms the permanent change from amorphous to a poly-crystalline state revealing *set* process of IST devices within a short pulse of 1.5 ns. Therefore, the present time-resolved experimental results of incubation-assisted switching shed light on achieving ultrafast crystallization via a weak electric field induced thermal pre-structural ordering. This approach also evidences realizing an extremely fast, yet low power threshold switching of IST devices.

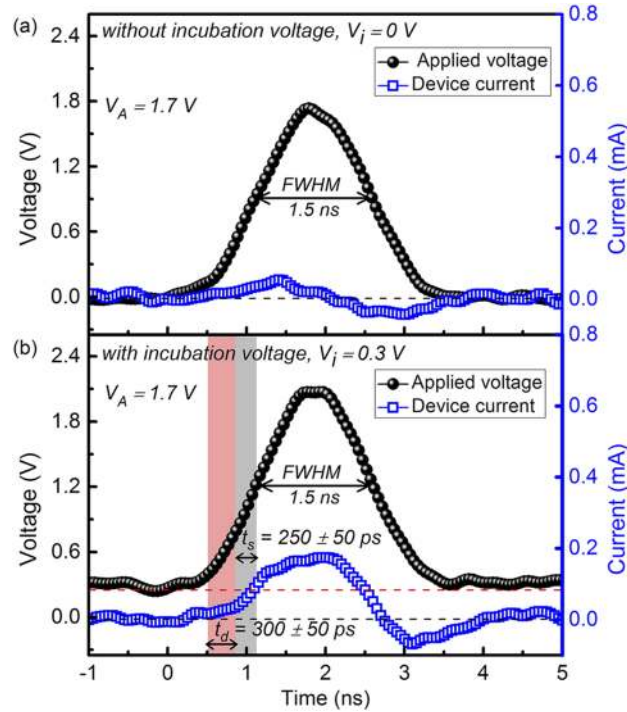


FIG. 4. Current-voltage characteristics of IST devices for the applied voltage pulse, V_A of 1.7 V with a full width half maxima (FWHM) pulse-width of 1.5 ns, rise time, and fall time of 1 ns (a) without incubation voltage, the device does not exhibit switching (b) with incubation voltage, reveals ultrafast *set* process of IST devices for the same V_A of 1.7 V within 1.5 ns.

In addition to showing rapid crystallization speeds, IST devices are known to possess better thermal stability ($T_c \sim 250^\circ C$) as compared to several GeSbTe, GeTe based PC materials.^{2,15,16} In the light of above, IST is certainly considered as one of the best candidates with greater technological importance not only for enabling PCM device with ps programming but also for multi-bit data storage²⁷ and ‘universal memory’ device.^{1,3,4}

IV. CONCLUSION

In conclusion, we have demonstrated ultrafast crystallization of IST devices by employing a weak electric field, (incubation voltage, V_i of 0.3 V) to the applied voltage pulse, V_A . This approach of incubation-assisted switching validates approximately one order faster threshold switching due to thermal prestructural ordering induced by Joule heating, with an extremely small delay time, t_d of 300 ps, as compared with no incubation voltage ($V_i = 0 V$) for the same V_A . The voltage-dependent incubation-assisted threshold switching dynamics confirms that the initiation of switching process proceeds even for 0.82 times of V_A , corroborating low power switching of IST devices. Furthermore, the incubation-driven ultrafast *set* process was achieved for V_A of a very short pulse-width of 1.5 ns and amplitude of 1.7 V, which is about 18% lower as compared to no incubation evidencing an extremely fast as well as low power *set* process of IST devices. These experimental findings would pave a way for designing of PCMs with low power and ultrafast programming speeds and also towards ‘universal memory’ for future computing.

ACKNOWLEDGMENTS

A.M. thanks the Department of Science and Technology (Grant number: SB/EMEQ-032/2013) and Department of Atomic Energy (Grant number: 2013/20/34/2/BRNS), Government of India for financial support. X-ray diffraction, FE-SEM experiments were performed at the Sophisticated Instrument Centre, Indian Institute of Technology Indore.

- ¹ M. Wuttig, *Nat. Mater.* **4**, 265 (2005).
- ² M. Wuttig and N. Yamada, *Nat. Mater.* **6**, 824 (2007).
- ³ M. H. R. Lankhorst, B. W. S. M. Ketelaars, and R. A. M. Wolters, *Nat. Mater.* **4**, 347 (2005).
- ⁴ D. Loke, T. H. Lee, W. J. Wang, L. P. Shi, R. Zhao, Y. C. Yeo, T. C. Chong, and S. R. Elliott, *Science* **336**, 1566 (2012).
- ⁵ F. Xiong, A. D. Liao, D. Estrada, and E. Pop, *Science* **332**, 568 (2011).
- ⁶ S. Lai and T. Lowrey, *Tech. Dig.—Int. Electron Devices Meet.* 36.5.1 (2001).
- ⁷ H. S. P. Wong, S. Raoux, S. B. Kim, J. Liang, J. P. Reifenberg, B. Rajendran, M. Asheghi, and K. E. Goodson, *Proc. IEEE* **98**, 2201 (2010).
- ⁸ W. Wang, L. Shi, R. Zhao, K. Lim, H. Lee, T. Chong, and Y. Wu, *Appl. Phys. Lett.* **93**, 043121 (2008).
- ⁹ S. R. Ovshinsky, *Phys. Rev. Lett.* **21**, 1450 (1968).
- ¹⁰ D. Adler, M. S. Shur, M. Silver, and S. R. Ovshinsky, *J. Appl. Phys.* **51**, 3289 (1980).
- ¹¹ K. D. Shukla, N. Saxena, S. Durai, and A. Manivannan, *Sci. Rep.* **6**, 37868 (2016).
- ¹² P. Zalden, M. J. Shu, F. Chen, X. Wu, Y. Zhu, H. Wen, S. Johnston, Z.-X. Shen, P. Landreman, M. Brongersma, S. W. Fong, H. S. P. Wong, M. J. Sher, P. Jost, M. Kaes, M. Salinga, A. V. Hoegen, M. Wuttig, and A. M. Lindenberg, *Phys. Rev. Lett.* **117**, 067601 (2016).
- ¹³ R. Simpson, P. Fons, A. Kolobov, T. Fukaya, M. Krbal, T. Yagi, and J. Tominaga, *Nat. Nanotechnol.* **6**, 501 (2011).
- ¹⁴ D. Loke, J. M. Skelton, W. J. Wang, T. H. Lee, R. Zhao, T. C. Chong, and S. R. Elliott, *PNAS* **111**, 13272 (2014).
- ¹⁵ G. Bruns, P. Merkelbach, C. Schlockermann, M. Salinga, M. Wuttig, T. Happ, J. Philipp, and M. Kund, *Appl. Phys. Lett.* **95**, 043108 (2009).
- ¹⁶ N. Yamada, E. Ohno, K. Nishiuchi, N. Akahira, and M. Takao, *J. Appl. Phys.* **69**, 2849 (1991).
- ¹⁷ Y. Maeda, H. Andoh, I. Ikuta, and H. Minemura, *J. Appl. Phys.* **64**, 1715 (1988).
- ¹⁸ Y. T. Kim, E. T. Kim, C. S. Kim, and J. Y. Lee, *Phys. Status Solidi (RRL)* **5**, 98 (2011).
- ¹⁹ Y. T. Kim and S. I. Kim, *Appl. Phys. Lett.* **103**, 121906 (2013).
- ²⁰ V. L. Deringer, W. Zhang, P. Rausch, R. Mazzarello, R. Dronskowski, and M. Wuttig, *J. Mater. Chem. C* **3**, 9519 (2015).
- ²¹ Y. I. Kim, E. T. Kim, J. Y. Lee, and Y. T. Kim, *Appl. Phys. Lett.* **98**, 091915 (2011).
- ²² E. T. Kim, J. Y. Lee, and Y. T. Kim, *Phys. Status Solidi (RRL)* **3**, 103 (2009).
- ²³ S. K. Pandey and M. Anbarasu, *Appl. Phys. Lett.* **108**, 233501 (2016).
- ²⁴ M. Anbarasu, M. Wimmer, G. Bruns, M. Salinga, and M. Wuttig, *Appl. Phys. Lett.* **100**, 143505 (2012).
- ²⁵ B.-S. Lee, G. W. Burr, R. M. Shelby, S. Raoux, C. T. Rettner, S. N. Bogle, K. Darmawikarta, S. G. Bishop, and J. R. Abelson, *Science* **326**, 980 (2009).
- ²⁶ P. K. Khulbe, E. M. Wright, and M. Mansuripur, *J. Appl. Phys.* **88**, 3926 (2000).
- ²⁷ A. Athmanathan, M. Stanisavljevic, N. Papandreou, H. Pozidis, and E. Eleftheriou, *IEEE J. Emerging Sel. Top. Circuits Syst.* **6**, 87 (2016).